NMR Solvent Shifts of Acetonitrile from Frozen Density Embedding Calculations

Rosa E. Bulo,* Christoph R. Jacob, and Lucas Visscher

Faculty of Sciences, Department of Theoretical Chemistry, Vrije Universiteit Amsterdam, De Boelelaan 1083, 1081 HV Amsterdam, The Netherlands

Received: November 5, 2007; In Final Form: January 3, 2008

We present a density functional theory (DFT) study of solvent effects on nuclear magnetic shielding parameters. As a test example we have focused on the sensitive nitrogen shift of acetonitrile immersed in a selected set of solvents, namely water, chloroform, and cyclohexane. To include the effect of the solvent environment in an accurate and efficient manner, we employed the frozen-density embedding (FDE) scheme. We have included up to 500 solvent molecules in the NMR computations and obtained the cluster geometries from a large set of conformations generated with molecular dynamics. For small solute−solvent clusters comparison of the FDE results with conventional supermolecular DFT calculations shows close agreement. For the large solute−solvent clusters the solvent shift values are compared with experimental data and with values obtained using continuum solvent models. For the water → cyclohexane shift the obtained value is in very good agreement with experiments. For the water → chloroform NMR solvent shift the classical force field used in the molecular dynamics simulations is found to introduce an error. This error can be largely avoided by using geometries taken from Car−Parrinello molecular dynamics simulations.

Introduction

NMR spectroscopy is among the most powerful and most extensively used tools for structure determination in chemistry today.[1] Because a wide variety of important compounds contain nitrogen (fine chemicals, natural products, and over 80% of all drugs) nitrogen NMR spectra (^{14,15}N) are of great value in this field. These spectra have an advantage over spectra of the generally more abundant ^{1}H and ^{13}C nuclei, namely that comprehensive results can be obtained in undeuterated solvents, or even in crude reaction mixtures, where due to the variety of compounds present ^{1}H and ^{13}C NMR spectroscopy would produce data that are impossible to interpret. Methods for the prediction of chemical shifts greatly aid not only in the interpretation of data but also in the measurement processes themselves, where the broad acquisition range of the chemical shift gives rise to a need for a priori knowledge.

Over the past decade, quantum chemical methods have become increasingly useful for NMR shift studies,[2,3] as they allow one to investigate structural and environmental effects in a systematic and controlled manner. However, due to the cost of the quantum chemical calculations involved, even at the efficient level of density functional theory (DFT), the system sizes accessible to such methods are severely limited. The study of solute−solvent interactions is especially difficult, because for a meaningful comparison of the theoretical and experimental data, one not only needs to include a large number of solvent molecules but also one needs to average over many different configurations to model a solution at finite temperature. Thorough studies were published using periodic boundary conditions in combination with plane wave calculations to obtain both an ensemble of solution geometries and NMR chemical shifts.[4] However, this approach requires quantum chemical calculations that are too demanding to carry out in a routine manner. In addition, the pseudopotential description of the atomic cores influences the accuracy of the NMR calculations. A marginally more efficient approach is to obtain the ensembles using classical molecular dynamics, or Monte Carlo techniques, followed by fully quantum chemical ground-state and NMR computations on sufficiently large solute−solvent clusters.[5,6] However, in this case the quantum chemical NMR computation is still very time-consuming, so that only a small number of solvent molecules can be included.

Including environment effects in more economical ways has been attempted in several different manners. Among the existing methods are mixed basis set methods,[7] which are less time-consuming than full basis-set methods but still require electronic structure calculations on the full system. More efficient, though more approximate approaches are combined quantum mechanics and molecular mechanics (QM/MM)[8] models,[9] in which the solute is treated with quantum chemical methods, whereas classical force fields are used to describe the solvent, as well as (part of) the solute−solvent interactions. This approach can be applied to both structure generation and NMR computation and makes the calculation of molecular properties for a large number of structures feasible. However, the force field used in the MM part has to be parametrized carefully, to accurately describe the solvent effect.

In continuum solvation models,[10] the solvent is described as a continuous medium that is characterized by its dielectric constant, with the solute molecule residing inside a cavity in this medium.[5] Since the atomistic structure of the solvent is not explicitly included in these continuum models, the averaging over different solvent configurations is implicit in the continuum description. Although it is clear that continuum models are able to correctly describe nonspecific solvation effects, i.e., dielectric

* Corresponding author. E-mail: bulo@few.vu.nl.

10.1021/jp710609m CCC: $40.75
Published on Web 02/27/2008

SCHEME 1: Schematic Representation of Acetonitrile Interacting with Water, Chloroform and Cyclohexane

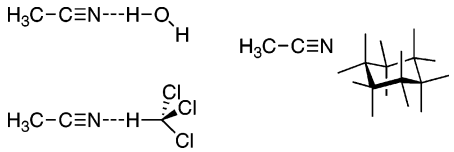

medium effects, their ability to describe specific interactions like hydrogen bonding is less obvious, requiring very careful parametrization of the size and shape of the cavity[11] or the explicit inclusion of a number of solvent molecules.[5]

Frozen density embedding (FDE) provides an efficient and fully ab initio quantum chemical way to compute solvent effects.[12,13] Recently, an extension to NMR computations has been developed and it has been shown that this approach accurately reproduces the results of conventional DFT calculations of the NMR chemical shift in bimolecular complexes of acetonitrile and a solvent molecule.[14] The core orbitals of the nucleus of interest are explicitly included, allowing a more accurate description of NMR parameters than the pseudopotential approach mentioned earlier. This method may open the way to routine calculations of environmental effects of NMR shieldings by allowing calculations on large solvent clusters in an efficient manner.

In this paper we will show that for large acetonitrile−solvent clusters the accuracy of FDE relative to conventional DFT calculations does still hold, and that we efficiently obtain values that can directly be compared with experimental results. We consider water and chloroform as examples of strongly interacting protic polar solvents and cyclohexane as an apolar solvent (Scheme 1). The shift in the NMR shielding when exchanging one solvent for the other can then be directly compared to experiment.

This work is organized as follows. In the Methods section the methods involved in obtaining the NMR solvent effects on NMR shielding are discussed in some detail. The Results section is divided into three parts. In part A the performance of the first principles and classical molecular dynamics simulations are discussed. In part B convergence behavior with ensemble and cluster size is discussed, in combination with timing statistics. In part C results are presented for solvent effects on the nitrogen shielding obtained from FDE calculations at cluster sizes with converged shielding values. For these computations, unpolarized frozen densities are used on the solvent molecules. Finally, in part D, the accuracy of the FDE method is assessed more directly, by comparing the results for small clusters with conventional DFT computations. This comparison was carried out for all three solutions investigated.

Methods

Frozen Density Embedding. Frozen density embedding (FDE) is a parameter-free method that optimizes the orbitals of an active subsystem I, in the presence of an embedding potential ($v_{\mathrm{eff}}^{\mathrm{emb}}$, eq 1)[12] induced by a frozen density (ρ_{II}, eq 1) that represents the solvent environment (subsystem II). This embedding potential (eq 2) contains the nuclear attraction and Coulomb electron repulsion, plus the functional derivative of the nonadditive parts of the exchange-correlation and kinetic energy of the two subsystems.

$$\left[-\frac{\nabla^2}{2} + v_{\mathrm{eff}}^{\mathrm{KS}}[\rho_{\mathrm{I}}](\vec{r}) + v_{\mathrm{eff}}^{\mathrm{emb}}[\rho_{\mathrm{I}},\rho_{\mathrm{II}}](\vec{r})\right]\varphi_i = \epsilon_i\varphi_i \qquad i = 1, ..., \frac{N_i}{2} \quad (1)$$

$$v_{\mathrm{eff}}^{\mathrm{emb}}[\rho_{\mathrm{I}},\rho_{\mathrm{II}}](\vec{r}) = v_{\mathrm{II}}^{\mathrm{nuc}}(\vec{r}) + \int \frac{\rho_{\mathrm{II}}(\vec{r}\,')}{|\vec{r} - \vec{r}\,'|}\,\mathrm{d}\vec{r}\,' + \frac{\delta E_{\mathrm{xc}}^{\mathrm{nadd}}[\rho_{\mathrm{I}},\rho_{\mathrm{II}}]}{\delta\rho_{\mathrm{I}}} + \frac{\delta T_{\mathrm{s}}^{\mathrm{nadd}}[\rho_{\mathrm{I}},\rho_{\mathrm{II}}]}{\delta\rho_{\mathrm{I}}} \quad (2)$$

With FDE, diagonalization of the Kohn−Sham matrix of the full system is avoided and replaced by separate computations of the densities of small subsystems, taken here as the solute and individual solvent molecules. Usually, it suffices to compute the frozen densities of the solvent molecules at further levels of approximation (no polarization, smaller basis sets, no GGA corrections) than the calculation of the active system.[13b] If needed, polarization of the frozen subsystems can be included, by relaxing the solvent densities in embedding calculations that consider as the frozen environment the solute and other solvent molecules (freeze-and-thaw cycles).[15]

Because in such a treatment the Kohn−Sham orbitals of the full system are not available, an approximate functional has to be applied for the kinetic energy component of the embedding potential. With the available kinetic energy functionals, accurate results can be obtained for a number of molecular properties, e.g., electronic absorption spectra,[13] ESR hyperfine coupling constants,[16] and induced circular dichroism spectra.[13] The FDE scheme has further been applied in molecular dynamics simulations[17] and free energy calculations.[18]

Calculation of NMR Shieldings with Frozen Density Embedding. The NMR chemical shifts were calculated by considering the perturbation of the orbitals due to an external magnetic field B in a basis of gauge including atomic orbitals (GIAO).[19,20] The chemical shielding can be expressed as a sum of diamagnetic and paramagnetic terms ($\sigma = \sigma_{\mathrm{d}} + \sigma_{\mathrm{p}}$). The former term depends only on the unperturbed electron density, whereas the second term takes into account the contribution from the first-order perturbation of the orbitals. Both terms can be expressed as a sum of contributions from the individual subsystems ($\sigma = \sigma_{\mathrm{d}}^{\mathrm{I}} + \sigma_{\mathrm{p}}^{\mathrm{I}} + \sigma_{\mathrm{d}}^{\mathrm{II}} + \sigma_{\mathrm{p}}^{\mathrm{II}}$).

Two approximations are made in the computation of the first-order perturbed orbitals and the resulting shielding values. As usual in DFT-NMR calculations we neglect the current dependence of the exchange−correlation functional and thereby also that of its nonadditive contribution to the embedding potential. In addition, we neglect the current dependence of the nonadditive kinetic energy functional. Previous calculations have furthermore shown that for nonaromatic solvents the shielding contribution from the frozen subsystem σ^{II} is negligible and can be omitted.[14]

In this work we mainly choose acetonitrile as the active (nonfrozen) subsystem, and consider increasingly large solute−solvent clusters in the FDE calculations to assess the error relative to a DFT treatment of the full system. We used the ADF program package[21] and the implementation of FDE in this package[15] for all DFT calculations. On the basis of earlier studies,[14,22] we chose to apply the PW91[23] kinetic energy functional to approximate the kinetic energy component of the embedding potential. In all FDE computations the molecular orbitals were expanded only in basis functions centered on the atoms of the nonfrozen system (FDE(m)).[22c,14]

For the active systems a triple ζ basis set with polarization functions (TZP) obtained from the ADF basis set library is used,

in combination with the local density approximation in the Vosko−Wilk−Nusair parametrization,[24] with nonlocal corrections for the exchange (Becke88) and correlation (Perdew 86) included.[32] The densities for the isolated solvent molecules were obtained in the local density approximation, with a double ζ basis set (DZP).

The large sets of calculations were processed using the PyADF program package.[25] This recently developed scripting framework allows the execution of workflows containing many subsequent ADF calculations and is based on the Python programming language.[26]

Molecular Dynamics. The NAMD classical molecular dynamics package[27] was used to obtain ensembles of configurations of acetonitrile in boxes of 30 Å in diameter, containing water, chloroform or cyclohexane as solvent. After equilibrating for 400 ps the system was evolved for a period of 2 ns. Every 2 ps a snapshot was extracted, for which NMR chemical shifts were then computed. We used the AMBER six-center force field for acetonitrile,[28] the TIP3P model for water,[29] and AMBER force fields[30] for chloroform and cyclohexane. For acetonitrile in chloroform and in cyclohexane we obtained additional configurational ensembles using first principles molecular dynamics (CPMD) on periodic boxes containing 32 solvent molecules. We used the CPMD program package,[31] with the BP86 exchange-correlation functional[32] and norm-conserving MT pseudopotentials[33] using the Kleinman-Bylander separation for the calculation of the nonlocal parts.[34] After equilibrating for 0.5 ps the system was evolved at room temperature for ca. 1 ps for the chloroform solution, and 0.5 ps for the cyclohexane solution. Every 10 fs a snapshot was extracted. We stress that in both molecular dynamics approaches discussed above, quantum mechanical effects on the motion of the nuclei are neglected. Especially very fast motions, such as intramolecular vibrations, are affected by this approximation, and this may cause an error in the absolute average nitrogen chemical shift. We are, however, interested in relative quantities only, and we assume that the error thus made cancels when we take the difference between the average chemical shifts in different solvents.[35] This assumption is supported by experimental vibrational spectra, which show that the C−N stretch frequency is affected very little by a change of solvent.[36]

All NMR values referenced hereafter are averages over the one hundred snapshots taken from the molecular dynamics simulations. The snapshots are sufficiently far apart in time to exclude correlation between subsequent configurations. The averages can readily be compared with experimental values, which reflect both a time and an ensemble average. In view of the sensitivity of the nitrogen chemical shift to the environment of the nucleus one needs to take care that the average NMR values are converged with respect to the number of snapshots used. Because part of the study involves analysis of the errors relative to a conventional DFT calculation, we extracted clusters of different sizes from the snapshots, selecting in each case the solvent molecules closest to the nitrogen atom of acetonitrile. Our largest FDE computations consist of one acetonitrile in a solvent cluster with a radius of 15 Å (corresponding to 500 water molecules).

Results and Discussion

A. Validation of the Molecular Dynamics Simulations. As described in the Methods section, we used both first principles and classical molecular dynamics simulations to obtain a set of geometries for the acetonitrile solutions. For these geometry ensembles we then extracted clusters of various sizes for which we computed the NMR shielding values. In this section we discuss the performance of both molecular dynamics methods. First, the accuracy of the CPMD method is discussed, by comparison of obtained vibrational frequencies with experiment. Subsequently the performance of the classical force field for the description of the potential energy surface is discussed, by comparing the obtained result with the presumably superior CPMD values.

We first computed the frequency of the C−N stretch vibration from our longest CPMD simulation (acetonitrile in chloroform) by directly Fourier transforming the velocity autocorrelation function of this motion. Smoothing of the spectra was done with the maximum entropy method. To the accuracy that our relatively short simulations can give for this time-dependent quantity, we found a very reasonable agreement with experimental values (exp 2255.8 cm^{-1},[36] CPMD $\sim$2170 cm^{-1}). A relatively long CPMD simulation of acetonitrile in the gas phase yielded almost the same frequency giving a gas to solvent shift of the vibrational frequency of 0 cm^{-1}, in complete agreement with the experimental observations.[36] These results indicate our CPMD simulations are reliable enough to allow direct comparison to experiment.

We then compared the geometries for the ensembles obtained from the CPMD simulation of acetonitrile in cyclohexane to those obtained with the more economical classical force field. The radial distribution functions (RDF) for the important intermolecular N−H interactions are in very good agreement for the two trajectories. The C−N bond parametrization in the force field does lead to an average intramolecular C−N bond length that is much shorter in the classical simulation than in the CPMD run ($\Delta R^{avg}_{C-N} = -0.02$ Å). Because the same parametrization is used in all classical MD calculations, this error should, however, not vary much between solvents and therefore not affect the relative values much. Furthermore, we observe that for any cluster size the average shielding values obtained from the classical and the CPMD calculations are significantly different, whereas the spread of the shift (calculated over a set of 100 snapshots) is similar, about 10 ppm in both cases. This indicates that this force field can indeed be used to represent solvent effects in this case. This assumption is further substantiated by considering the gas to solvent shift of the average C−N bond length, which is crucial for a correct representation of the solvent effects on the NMR shielding. In the CPMD simulations, the presence of the solvent shortens the average C−N bond length by 0.0020 Å, compared to a shortening of 0.0024 Å induced by the classical solvent.

In summary, we have shown that CPMD simulations are able to describe the behavior of an acetonitrile solution to high accuracy, and that the solvent effect on the intramolecular CN distance in acetontrile can be sufficiently well described by a classical force field.

B. Convergence of Ensemble-Size, Cluster-Size, and Timing Statistics. A reliable estimate of the NMR chemical shift of a solvated molecule can only be obtained if the calculation is converged with respect to cluster size and with respect to the number of configurations taken in the average. The first issue will be discussed in more detail in section C. The convergence with respect to the number of configurations taken is displayed in Figure 1. On the basis of these data we concluded that 100 snapshots from the molecular dynamics simulation are sufficient to obtain converged mean values. We thereby note that the standard deviation of the set of shielding values lies in the range of 10 ppm, which is the same order of magnitude as the solvent shifts of the shielding values themselves (Figure S1 of Sup-

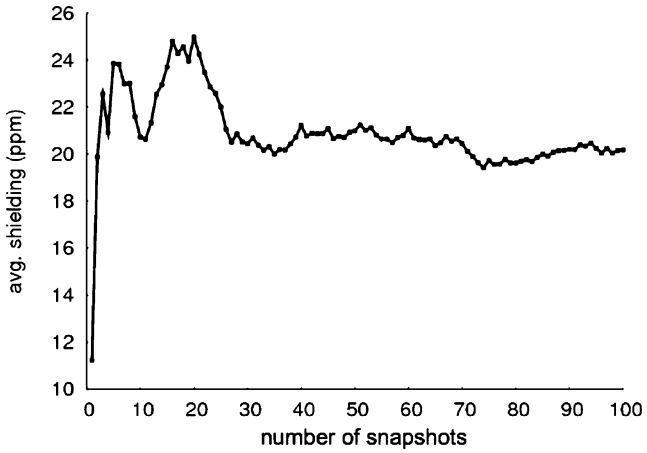

Figure 1. Convergence of average shielding value with the number of configurations for a cluster of 500 water molecules, treated with FDE.

porting Information). This illustrates once more that use of a single configuration may easily yield meaningless results.

Convergence studies (further discussed in section C) with respect to cluster size show that the average shielding values for the aqueous solution are converged at a cluster radius of about 11 Å (200 water molecules, Figure 2a). Figure 2b shows the average timings of the single point and NMR calculations using FDE and conventional DFT on systems containing one acetonitrile molecule (active system) in water clusters of varying sizes (fully frozen in the FDE calculation). The large speed-up clearly shows the advantage of the presented method, and also illustrates that the larger cluster sizes can be considered out of reach for conventional DFT calculations.

C. Solvent Effects of Water, Chloroform, and Cyclohexane on the Nitrogen Shielding Value of Acetonitrile. In this section we discuss solvent effects on the NMR shielding values using FDE and compare to the available experimental solvent-to-solvent data. An alternative comparison could in principle be made with experimental gas-to-solvent shifts, but though such values are easily obtained computationally, the experimental procedures to calculate such shifts contain so many uncertainties and approximations that we deem them not reliable enough to provide benchmark data for our method.

The most simple and efficient way of constructing the frozen solvent environment required in the FDE calculations is to superimpose the densities obtained from single point calculations on isolated solvent molecules at the LDA level using a small DZP basis set.[15] For the computation of the aqueous solutions, given the fact the water structure is fixed in the TIP3P model, this requires calculation of only a single water density.

The convergence of the average shielding values thus obtained with cluster size is depicted in Figure 3. The Figure shows that of the three solvents water has the largest effect on the chemical shielding, as can be expected, due to its strong hydrogen bonding interaction with the nitrogen lone pair. Analysis of the conformations shows that as many as three or four water molecules directly interact with the nitrogen center. For the chloroform and cyclohexane solutions faster convergence with the number of solvent molecules is observed. This fast convergence is partly due to the greater size of the solvent molecules, which is reflected in the coordination of no more than two chloroform molecules to the nitrogen atom of acetonitrile. In the aprotic cyclohexane solution barely any solute−solvent interaction can be discerned, as is reflected by the negligible influence of the solvent molecules on the chemical shielding.

Indirect solvent effects on the acetonitrile geometry are computed for the three different solvents by comparing shielding values computed for a single acetonitrile molecule at geometries taken from both the gas phase and the solution ensembles. For water and chloroform these shifts are respectively −4.1 and −5.1 ppm, signifying a stronger solvent effect on the intramolecular interactions than found in cyclohexane (−0.5 ppm). These values demonstrate that part of the observed solvent shift is due to the induced structural changes within the solute.

The converged solvent-to-solvent shift of 20.8 ppm for cyclohexane to water is in close agreement with the experimental value of 19.7 ppm (Table 1). This is a significant improvement of the results obtained with a continuum model, which underestimates the solvent shift by overestimating the acetonitrile−cyclohexane interaction.[5] Comparison of the cyclohexane to chloroform shift ($\Delta\sigma^{FDE} = 3.5$ ppm) to experimental data[37] reveals that the calculation severely underestimates this change ($\Delta\sigma^{exp} = 8.8$ ppm). The continuum solvent model does in this case reproduce the experimental value, but as is noted in the respective paper, this is due to a cancellation of errors caused by an overestimation of the interaction with both solvents.[5]

To analyze the error made for the cyclohexane-to-chloroform shift, we decided to check the quality of the structures generated with molecular dynamics. The RDFs for acetonitrile in water compare well with previously published values[38] and appear to describe the N···H hydrogen-bonding sufficiently well. Standard

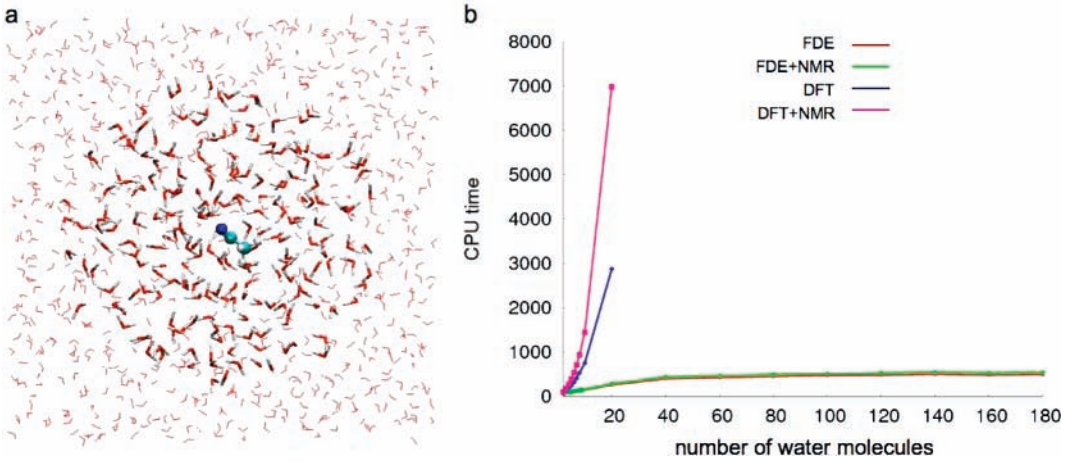

Figure 2. (a) Illustration of acetonitrile in water cluster. (b) Timing statistics for frozen density embedding single point (FDE) and NMR (FDE+NMR) calculations and for the conventional DFT calculation (DFT and DFT+NMR) of acetonitrile in the presence of increasingly large clusters of water molecules.

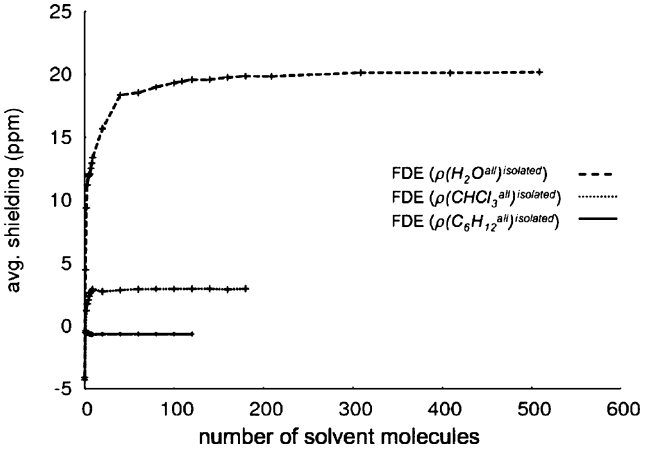

Figure 3. Convergence of the FDE chemical shielding values for acetonitrile in water, chloroform and cyclohexane with cluster size, relative to the gas-phase value.

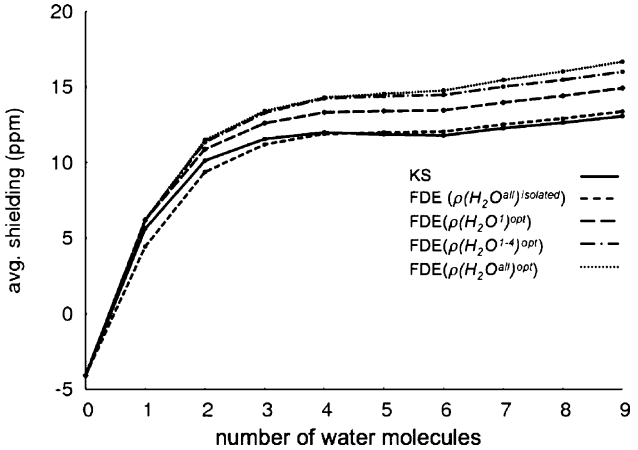

Figure 4. Average shielding value of the nitrogen nucleus in the presence of different numbers of water molecules. The values are relative to the absolute gas-phase value of −18.20 ppm.

TABLE 1: Comparison of the FDE Solvent Shifts with Experimental Values

$\Delta\sigma$(N)	FDE^{MM}	FDE^{CPMD}	continuum	exp
$C_6H_{12} \rightarrow H_2O$	20.8[a]		14.4[b]	19.7[c]
$C_6H_{12} \rightarrow CHCl_3$	3.5[a]	11.6[a]	7.9[b]	8.8[c]

[a] For clusters with a radius of 15 Å. [b] Reference 5. [c] Reference 37.

force fields like the ones used here, however, are less well calibrated for nonaqueous solutions and could lead to a systematic error in the generated structures. We compared the classical RDF with CPMD generated structures for acetonitrile in chloroform, and found peaks at N···H distances of 2.5 and 2.3 Å, respectively. This suggests that the average N···H hydrogen bond distance is overestimated by a few tenths of angstroms in the classical simulation. We therefore conclude that our classical ensemble of structures does probably underestimate the interaction between the acetonitrile and the chloroform molecules. This error should be remedied by taking the structures for the NMR calculation from the CPMD simulations, and we do indeed observe that the shift in the cyclohexane-to-chloroform shielding value ($\Delta\sigma = 11.6$ ppm) is in considerably better agreement with experiment ($\Delta\sigma = 8.8$ ppm). This improvement is entirely due to the chloroform simulation, because, as mentioned in section A, the RDFs for acetonitrile with cyclohexane obtained from a CPMD simulation are almost identical to the force field results.

D. Comparison with Conventional DFT Calculations. To assess the accuracy of the FDE approximation itself, we compare the obtained FDE results for small clusters to conventional DFT calculations.[39] The obtained error can result from the approximate kinetic energy functional used in the computation of the ground-state density, as well as from the additional approximations made in the calculation of NMR shieldings using FDE, i.e., the neglect of the current-dependence of the nonadditive kinetic energy and the neglect of the induced current in the environment (see the Introduction and ref 14). Additional sources of error are the approximations used in the construction of the frozen environment density. To minimize these errors and to identify the intrinsic errors of the FDE treatment, we performed a systematic analysis using frozen densities obtained at different levels of approximation.

Using the set of 100 snapshots obtained from the molecular dynamics simulations, the conventional DFT and FDE average nitrogen shielding values were computed for small solute−solvent clusters of different sizes, containing at maximum nine solvent molecules, which are as many as was feasible in the reference supermolecular conventional DFT calculations. In this manner the influence of the rest of the solvent environment is indirect and incomplete because it only affects the cluster structures. The direct contribution to the shielding values is taken into account solely for the solvent molecules within the selected cluster.

Acetonitrile in Water. In the calculation of the water clusters an overall increase in the absolute value of the shielding can be seen upon enlargement of the cluster, as depicted in Figure 4. The FDE results were obtained using the most simple and efficient manner to compute the NMR shielding values, where one superimposes the densities obtained from single point calculations on isolated water molecules using LDA and a small DZP basis set. The resulting shielding values as a function of the number of water molecules are depicted as a dashed line. The conventional DFT results are very well reproduced, with average errors of ca. 1 ppm.

We then performed additional calculations in which we allowed one or more water molecules to polarize in a single freeze-and-thaw cycle. In all cases, this polarization results in further increase of the shielding value of the nitrogen nucleus, but only for clusters containing one or two water molecules does this bring the results in closer agreement with the conventional DFT result. For larger clusters inclusion of polarization in FDE freeze−thaw cycles increases the error. Polarization of all water molecules in the largest cluster, a full first solvation shell, results in the largest shielding value and the largest deviation from the conventional DFT value ($\Delta\Delta\sigma = 3.6$ ppm for the fully polarized system). The average and rmsd errors are presented in the Supporting Information (Table S1).

This large error shows that error cancellation is partly responsible for the good agreement found in the FDE calculations using an unpolarized environment. It turns out that in this case, the error introduced by the approximate environment density cancels the error introduced by other approximations made in the FDE treatment, in particular those due to the use of an approximate kinetic energy functional. If the former error is removed by using a more accurate, polarized density for the environment, the intrinsic errors of the FDE treatment are revealed. To investigate these errors in more detail, we investigated the effects of the environment on the diamagnetic and the paramagnetic contributions to the shielding separately.

The downfield shift in the shielding value upon enlargement of the cluster corresponds to a deshielding of the nucleus. This

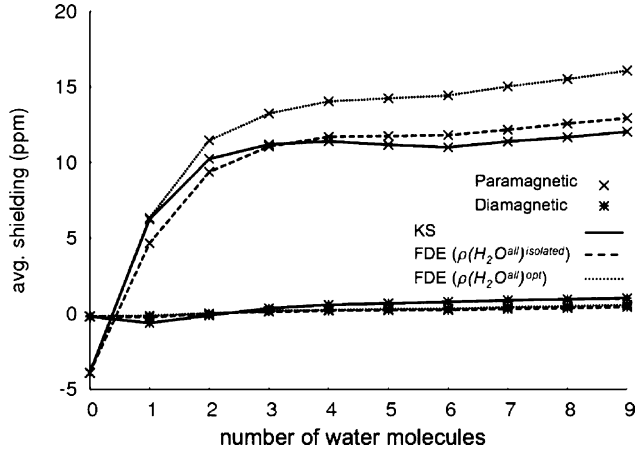

Figure 5. Diamagnetic and the paramagnetic shielding contributions for the conventional DFT and the FDE calculations. The values are relative to the gas-phase value (paramagnetic (g), −349.19; diamagnetic (g), 331.00).

effect may either be attributed to a diminished electron density on of the nitrogen atom (electron donation to the water molecules) or be related to the induced current stemming from the perturbed orbitals. The contributions of the diamagnetic and the paramagnetic shielding values given in Figure 5 show that the latter term is the main cause of the observed effect.

Figure 5 shows how for the unpolarized result (dashed line) both the paramagnetic and the diamagnetic term agree well with the conventional DFT values (solid line), but for very small errors in opposite directions. Polarization of the densities through freeze−thaw cycles (dotted line) has very little effect on the diamagnetic term, whereas the deviation from the conventional DFT value of the paramagnetic contribution increases considerably. The total error introduced upon polarization must therefore be related to the perturbation calculation. Figure 5 indicates that polarization of the frozen densities gives a minor improvement in the diamagnetic term. The quality of the produced electron density is directly related to the error in this term, and to confirm its improvement by polarization, the effect of the FDE method on the density itself will be discussed in the following.

Visualization of the electron density on acetonitrile of a representative snapshot obtained with the various methods (Figure 6, transparent surface) shows three very similar electron densities, which is in agreement with the small differences found in the diamagnetic shielding terms. To visualize the effect of the water molecules on the acetonitrile electron density with the different methods, we plotted the density change upon addition of a fifth water molecule (yellow) to a cluster containing four coordinated water molecules (nontransparent blue lobes indicate an increase in electron density, and nontransparent green lobes indicate a decrease). The fifth water molecule does not coordinate directly to acetonitrile but forms a hydrogen bond with an already coordinated water molecule (no. 2). In doing so, the interaction of water molecule 2 with acetonitrile is reduced, and electron donation from the nitrogen atom toward water 2 decreases. This is reflected by the negative (green) density change along the hydrogen bond in the conventional DFT computation. A similar result is seen from the FDE density obtained with the isolated frozen densities, but to a lesser extent, because the fifth water molecule does not polarize the first solvation shell. When polarization of the frozen densities is taken into account, the density change becomes very similar to the Kohn−Sham result. The positive effect of polarization on the electron density is thus in agreement with the improvement of the diamagnetic shielding term.

The combined results for small acetonitrile−water clusters show a satisfactory agreement with the conventional DFT benchmark (1−3 ppm). In addition, the results clearly suggest that any deviations from the benchmark stem from the approximations made in the computation of the paramagnetic term, whereas the diamagnetic term is very well represented. This means that the effect on the ground-state electron density is described accurately, whereas the description of the virtual orbitals and their orbital energies, which is crucial for the calculation of the induced current, is less reliable.

Acetonitrile in Chloroform and Cyclohexane. For small clusters of acetonitrile in chloroform solution, the results are very similar to those of acetonitrile−water clusters. For up to two solvent molecules the average FDE shielding values compare very well to conventional DFT results, but at larger cluster sizes an error of 1.3 ppm appears. As in the acetonitrile−water clusters the inclusion of polarization effects on the solvent molecules causes a downfield shift. The errors (values are given in the Supporting Information, Table S2) are similar to those of the water clusters, particularly if one takes into consideration the larger volume of the chloroform molecules. For clusters of nine chloroform molecules the error appears to reach a stable value (maximum 4.5 ppm for the fully polarized system).

In cyclohexane the nitrogen shielding of acetontrile remains similar to the gas-phase value for all cluster sizes (see Supporting Information Table S3). The result is not very sensitive to the size of the cluster chosen and contrary to the effect of the other solvents, the conventional DFT results show a modest upfield shift (∼−0.5 ppm). The FDE results are very similar but show a small downfield shift (∼0.2 ppm).

Improvement of the Error Introduced by the FDE Approximation. A standard way to circumvent the errors introduced by the inaccuracies in the FDE description of the solute−solvent interaction is to include the most strongly interacting solvent molecules in the solute calculation, i.e., to include one or more of the solvent molecules in the active subsystem. To study the convergence of this procedure, we analyzed the root-

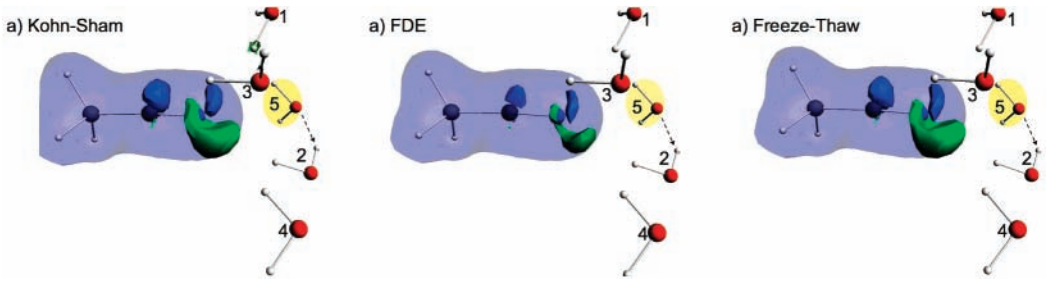

Figure 6. Electron density on acetonitrile (transparent), and the change upon addition of the fifth (yellow) water molecule (blue lobes positive; green lobes negative), for (a) a conventional DFT calculation, (b) an FDE calculation without polarization and (c) an FDE calculation with polarization of the water molecules included through freeze−thaw cycles.

TABLE 2: RMSD of FDE Results from Conventional DFT Calculation for a Cluster of Acetonitrile in 20 Water Molecules, at Different Sizes of the Active System

no. of H_2O included in solute system	RMSD from DFT (ppm) no. of additional polarized H_2O	
	0 H_2O	1 H_2O
0	2.36	2.39
1	2.07	2.30
2	1.96	2.06
3	1.79	1.84
4	1.45	1.46
5	1.39	1.36

mean-square deviations (rmsd) from the conventional DFT results for a cluster of twenty water molecules, with different numbers of active solvent molecules.

The error depicted in Table 2 is the average of the absolute (rmsd) deviations from the conventional DFT values for each of the 100 configurations. The densities of the frozen water molecules were obtained from isolated molecule LDA calculations with small basis sets, as before. As expected, this result shows a substantial decrease in the error for larger unfrozen regions, although additional polarization of the frozen densities still results in a modest increase in the error. Only when five water molecules are included in the nonfrozen region does polarization lead to an improvement of the final result.

Conclusions

Solvent effects on acetonitrile NMR chemical shielding values can be computed with good accuracy using the frozen density embedding description in an ensemble-averaged microsolvated model of the solvent. Intrinsic errors come from two sources, the classical molecular dynamics used to obtain the ensemble structures and the frozen density embedding approximation used for the solvent molecules. The latter approximation gives a small error of a few ppm. The structural errors depend on the accuracy of the applied force field and can be more substantial. This type of errors can be largely avoided by employing the more expensive but more accurate CPMD method to generate the ensemble of configurations.

In general the FDE results display a downfield shift (deshielding) with respect to the reference conventional DFT values. Deviations from this benchmark result become more pronounced when polarization effects are taken into account. The error is demonstrated to arise from the paramagnetic contribution to the shielding, and is probably due to errors made in the description of the virtual orbitals in the FDE procedure. Nevertheless, as the good agreement with experiment of the solvent-to-solvent shift values for the water → cyclohexane exchange shows, these systematic errors cancel for different solvents, making FDE a useful tool for the prediction of relative chemical shifts.

Finally we note that it has been shown previously that in conventional DFT calculations the orbitals[40,41] and NMR chemical shifts[42] can be improved significantly by employing the SAOP potential instead of a GGA potential. Introduction of the SAOP[43] potential in FDE NMR computations is also possible but complicates the error analysis of the FDE approximation,[14] which is why we have not considered this functional in the current study. In future work we plan to explore the performance of this combination in more detail.

Acknowledgment. We thank The Netherlands Organization for Scientific Research (NWO) for financial support and gratefully acknowledge computer time provided by the Foundation for Dutch Computing Facilities (NCF).

Supporting Information Available: Tables containing relative chemical shifts and average and rmsd errors relative to the conventional DFT results. Figure showing the spread of the NMR shileding values. This information is available free of charge via the Internet at http://pubs.acs.org.

References and Notes

(1) *NMR and Chemistry: An introduction to modern NMR spectroscopy*; Akitt, J. W., Mann, B. E., Eds.; CRC Press: London, U.K., 2000.

(2) *Calculation of NMR and EPR Parameters. Theory and Applications*; Kaupp, M., Bühl, M., Malkin, V. G., Eds.; Wiley-VCH: Weinheim, 2004.

(3) Helgaker, T.; Jaszunski, M.; Ruud, K. *Chem. Rev.* **1999**, *99*, 293−352.

(4) (a) Vaara, J. *Phys. Chem. Chem. Phys.* **2007**, *9*, 5399−5418. (b) Murakhtina, T.; Heuft, J.; Meijer, E. J.; Sebastiani, D. *ChemPhysChem* **2006**, *7*, 2578−2584.

(5) (a) Searles, D. B.; Huber, H. *Encyclopedia of Nuclear Magnetic Resonance, Volume 9: Advances in NMR*; Grant, D. M., Harris, R. K., Eds.; John Wiley & Sons: Chichester, U.K., 2002. (b) Mennucci, B.; Martinez, J. M.; Tomasi, J. *J. Phys. Chem. A* **2001**, *105*, 7287−7296. (c) Mennucci, B. *J. Am. Chem. Soc.* **2002**, *124*, 1506−1515

(6) Malaspina, T.; Coutinho, K.; Canuto, S. *J. Chem. Phys.* **2002**, *117*, 1692−1699.

(7) Moon, S.; Case, D. A. *J. Comput. Chem.* **2006**, *27*, 825−836.

(8) (a) Warshel, A.; Levitt, M. *J. Mol. Biol.* **1976**, *103*, 227−249. (b) Thole, B. T.; Van Duijnen, P. Th. *Theor. Chim. Acta* **1980**, *55*, 307−318. (c) Field, M. J.; Bash, P. A.; Karplus, M. *J. Comput. Chem.* **1990**, *11*, 700−733. (d) Gao, J. In *Reviews in Computational Chemistry*; Lipkowitz, K. B., Boyd, D. B., Eds.; VCH: New York, 1995; Vol. 7, pp 119−185. (e) Sherwood, P. In *Modern Methods and Algorithms of Quantum Chemistry*; Grotendorst, J., Ed.; Vol. 1 of NIC Series; John von Neumann Institute for Computing: Jülich, Germany, 2000; pp 257−277.

(9) (a) Komin, S.; Gossens, C.; Tavernelli, I.; Rothlisberger, U.; Sebastiani, D. *J. Phys. Chem. B* **2007**, *111*, 5225−5232. (b) Aidas, K.; Møgelhøj, A.; Kjær, H.; Nielsen, C. B.; Mikkelsen, K. V.; Ruud, K.; Christiansen, O.; Kongsted, J. *J. Phys. Chem. A* **2007**, *111*, 4199−4210.

(10) (a) Cramer, C. J.; Truhlar, D. G. *Chem. Rev.* **1999**, *99*, 2161−2200. (b) Tomasi, J.; Mennucci, B.; Cammi, R. *Chem. Rev.* **2005**, *105*, 2999−3094. (c) Tomasi, J.; Persico, M. *Chem. Rev.* **1994**, *94*, 2027−2094.

(11) Tomasi, J. *Theor. Chem. Acc.* **2004**, *112*, 184−203.

(12) (a) Wesolowski, T. A.; Warshel, A. *J. Phys. Chem.* **1993**, *97*, 8050−8053. (b) Wesolowski, T. A. in *Computational Chemistry: Reviews of Current Trends*, edited by Leszcynski, J. World Scientific, Singapore 2006, Vol. 10.

(13) (a) Jacob, C. R.; Neugebauer, J.; Jensen, L.; Visscher, L. *Phys. Chem. Chem. Phys.* **2006**, *8*, 2349−2359. (b) Neugebauer, J.; Louwerse, M. J.; Baerends, E. J.; Wesolowski, T. A. *J. Chem. Phys.* **2005**, *122*, 094115. (c) Neugebauer, J.; Jacob, C. R.; Wesolowski, T. A.; Baerends, E. J. *J. Phys. Chem. A* **2005**, *109*, 7805−7814. (d) Neugebauer, J. *J. Chem. Phys.* **2007**, *126*, 134116.

(14) Jacob, C. R.; Visscher, L. *J. Chem. Phys.* **2006**, *125*, 194104.

(15) Jacob, C. R.; Neugebauer, J.; Visscher, L. *J. Comput. Chem.* **2008**, DOI: 10.1002/jcc.20861.

(16) (a) Neugebauer, J.; Louwerse, M. J.; Belanzoni, P.; Wesolowski, T. A.; Baerends, E. J. *J. Chem. Phys.* **2005**, *123*, 114101. (b) Wesolowski, T. A.; Weber, J. *Chem. Phys. Lett.* **1996**, *248*, 71−76.

(17) Ianuzzi, M.; Kirchner, B.; Hutter, J. *Chem. Phys. Lett.* **2006**, *421*, 16−20.

(18) (a) Strajbl, M.; Hong, G.; Warshel, A. *J. Phys. Chem. B* **2002**, *106*, 13333−13343. (b) Olsson, M. H. M.; Hong, G.; Warshel, A. *J. Am. Chem. Soc.* **2003**, *125*, 5025−5039.

(19) v. Wüllen, C. In *Calculation of NMR and EPR Parameters. Theory and Applications*; Kaupp, M., Bühl, M., Malkin, V. G., Eds.; Wiley-VCH: Weinheim, 2004; pp 43−82.

(20) (a) Ditchfield, R. *Mol. Phys.* **1974**, *27*, 789−807. (b) Schreckenbach, G.; Ziegler, T. *J. Phys. Chem.* **1995**, *99*, 606−611.

(21) (a) ADF, Amsterdam density functional program, Theoretical Chemistry, Vrije Universiteit, Amsterdam, 2006; http://www.scm.com. (b) te Velde, G.; Bickelhaupt, F. M.; Baerends, E. J.; Fonseca Guerra, C.; van Gisbergen, S. J. A.; Snijders, J. G.; Ziegler, T. *J. Comput. Chem.* **2001**, *22*, 931−967.

(22) (a) Wesolowski, T. A.; Chermette, H.; Weber, J. *J. Chem. Phys.* **1996**, *105*, 9182−9190. (b) Wesolowski, T. A.; Ellinger, Y.; Weber, J. *J. Chem. Phys.* **1998**, *108*, 6078−6083. (c) Wesolowski, T. A. *J. Chem. Phys.* **1997**, *106*, 8516−8526.

(23) Lembarki, A.; Chermette, H. *Phys Rev. A* **1994**, *50*, 5328−5331.

(24) Vosko, S. H.; Wilk, L.; Nusair, M. *Can. J. Phys.* **1980**, *58*, 1200−1211.
(25) Jacob, C. R.; Bulo, R. E.; Visscher, L. Manuscript in preparation.
(26) http://www.python.org/.
(27) Kalé, L.; Skeel, R.; Bhandarkar, M.; Brunner, R.; Gursoy, A.; Krawetz, N.; Phillips, J.; Shinozaki, A.; Varadarajan, K.; Schulten, K. *J. Comput. Phys.* **1999**, *151*, 283−312.
(28) Grabuleda, X.; Jaime, C.; Kollman, P. A. *J. Comput. Chem.* **2000**, *21*, 901−908.
(29) Jorgensen, W. L.; Chandrasekhar, J.; Madura, J. D.; Impey, R. W.; Klein, M. L. *J. Chem. Phys.* **1983**, *79*, 926−935.
(30) (a) Wang, J.; Kollman, P. A. *J. Comput Chem.* **2001**, *22*, 1219−1228. (b) Weiner, S. J.; Kollman, P. A.; Nguyen, D. T.; Case, D. A. *J. Comput. Chem.* **1986**, *7*, 230−252.
(31) (a) Hutter J. et al. Computer code CPMD version 3.11.1, 1990−2005, Copyright IBM Corp. and MPI-FKF Stuttgart; http://www.cpmd.org. (b) Hutter, J.; Curioni, A. *ChemPhysChem* **2005**, *6*, 1788−1793. (c) Marx, D.; Hutter, J. Ab-initio molecular dynamcs: Theory and implementation. In *Modern Methods and Algorithms of Quantum Chemistry*; Grotendorst, J., Ed.; Vol. 1 of NIC Series; John von Neumann Institute for Computing: Jülich, Germany, 2000; pp 301−449.
(32) (a) Becke, A. D. *Phys. Rev. A* **1988**, *38*, 3098−3100. (b) Perdew, J. P. *Phys. Rev. B* **1986**, *33*, 8822−8824.
(33) Troulliers, N.; Martins, J. L. *Phys. Rev. B* **1991**, *43*, 1993−2006.
(34) Kleinman, L.; Bylander, D. M. *Phys. Rev. Lett.* **1982**, *48*, 1425−1428.
(35) Pennanen, T. S.; Vaara, J.; Lantto, P.; Sillanpää, A. J.; Laasonen, K.; Jokisaari, J. *J. Am. Chem. Soc.* **2004**, *126*, 11093−11102.
(36) Reimers, J. R.; Hall, L. E. *J. Am. Chem. Soc.* **1999**, *121*, 3730−3744.
(37) Witanowski, M.; Stefaniak, L.; Webb, G. A. In *Annual Report on NMR Spectroscopy*; Webb, G. A., Ed.; Academic Press: London, 1993; Vol. 25, p 212.
(38) Bakó, I.; Megyes, T.; Grósz, T.; Pálinkás, G.; Dore, J. *J. Mol. Liq.* **2006**, *125*, 174−180.
(39) Jacob, C. R.; Wesolowski, T. A.; Visscher, L. *J. Chem. Phys.* **2005**, *123*, 174104.
(40) Chong, D. P.; Gritsenko, O. V.; Baerends, E. J. *J. Chem. Phys.* **2002**, *116*, 1760−1772.
(41) Görling, A. *J. Chem. Phys.* **2005**, *123*, 062203.
(42) Poater, J.; van Lenthe, E.; Baerends, E. J. *J. Chem. Phys.* **2003**, *118*, 8584−8593.
(43) Gritsenko, O. V.; Schipper, P. R. T.; Baerends, E. J. *Chem. Phys. Lett.* **1999**, *302*, 199−207.